Simplified Analysis Technique for the Initial Design of LTCC Filters With All-Capacitive Coupling

K. Rambabu and Jens Bornemann, *Fellow, IEEE*

Abstract—The paper proposes a new low-temperature co-fired ceramic (LTCC) filter configuration, which improves the stopband behavior of previous designs by using all-capacitive couplings. Moreover, a simplified analysis technique is presented to aid filter engineers in the initial design of capacitively coupled LTCC resonators. Relationships from well-known conformal mapping expressions are used to model individual parts of the filter, which are combined by standard two-port parameters. This technique is shown to agree well with measurements of previously published filters. The proposed filter configuration is then verified by results obtained with different commercially available field solvers.

Index Terms—Bandpass filters, comb-line filters, computer-aided design, low-temperature co-fired ceramic (LTCC) filters, stepped-impedance resonators (SIRs).

I. INTRODUCTION

RF AND microwave system-on-chip (SOC) modules for wireless communications are increasingly fabricated in low-temperature co-fired ceramic (LTCC) technology, e.g., [1] and [2]. Filter components with transmission zeros are integral parts of the design methodology, and several designs have been presented, e.g., [3]–[5].

In [3], two stripline stepped-impedance resonators (SIRs) are coupled electromagnetically to form a single attenuation pole, which can be controlled through a planar line on a layer beneath the SIRs [4]. A two-pole filter with two attenuation poles, one on either side of the passband, has been developed based on inductively coupled resonators with a feedback capacitance between input and output [5]. However, the attenuation of this filter toward higher frequencies is rather poor.

The purpose of this paper is twofold: first, we propose a filter configuration with improved performance in the stopband. It is based on all capacitively coupled strips with two stripline SIRs and utilizes coupling from source to load, as well as from source/load to both SIRs. Two attenuation poles are created on either side of the passband, and their locations can be controlled by varying the coupling capacitances.

Secondly, we present a simplified analysis of capacitively coupled stripline components in LTCC, which permits the design engineer to perform a fast initial design of this class of LTCC filters.
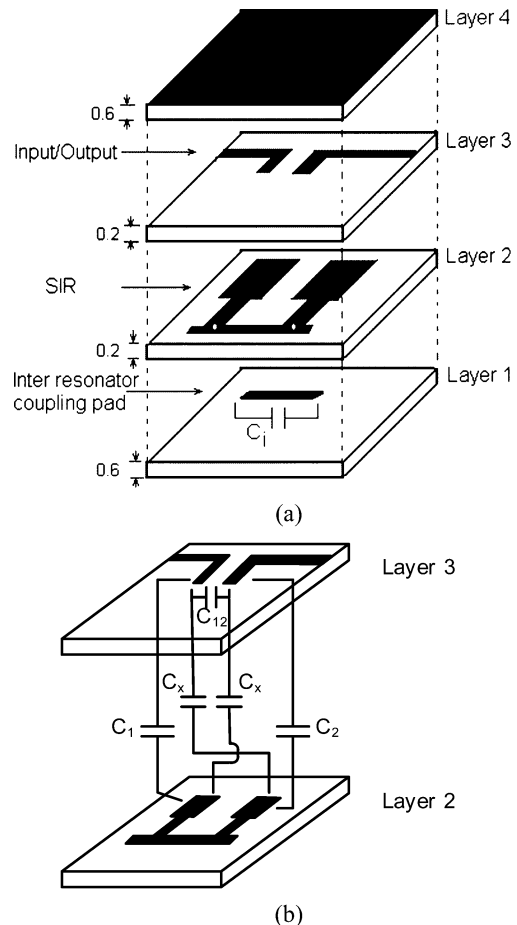
Fig. 1. (a) Proposed filter structure and (b) capacitors involved in the coupling scheme (layer thicknesses in millimeters).

II. FILTER STRUCTURE

Fig. 1(a) shows the schematic of the proposed filter including the capacitance for the inter resonator coupling pad. Fig. 1(b) depicts the remaining capacitances between layers 2 and 3.

Four layers of dielectrics are sandwiched between two ground planes. The SIRs are located on layer #2 and are shorted by via-holes at one end [white dots in Fig. 1(a)]. The input/output pads are printed on layer #3. The orientation and shape of these pads must simultaneously satisfy the source/load capacitance C_{12} and input/output capacitances C_1 and C_2. The cross-coupling between the input/output pad and the second/first resonator, which is represented by C_x in Fig. 1(b), is very crucial for the locations of the attenuation poles. Without these cross couplings, i.e., with only source/load capacitance
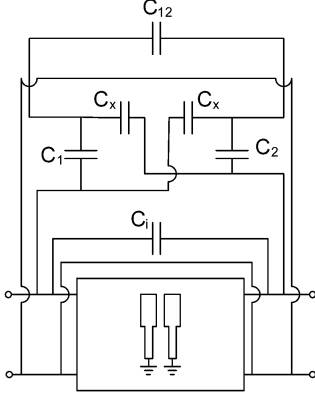
Fig. 2. Equivalent circuit of the filter structure in Fig. 1.

C_{12} in place, the attenuation poles would be positioned symmetrically about the passband. An external coupling pad is provided on layer #1 for additional control of the inter-resonator coupling via capacitance C_i. Note that contrary to the design in [3], the presence of C_i is not related here to the creation of transmission zeros, which are mainly produced by source–load coupling.

Other capacitances to be considered, in theory, are those from circuit elements to ground. However, substrate layers with a ground plane are usually thicker than those of inner layers [by a factor of three in Fig. 1(a)]. Therefore, and in order to keep the model simple, the ground capacitances are neglected here.

III. THEORY

According to Fig. 2, a matrix representation of the entire circuit can be obtained by adding the admittance matrices of the parallel-coupled lines and the inter-resonator capacitance C_i, converting to impedance and adding the impedance matrix of the block containing C_1, C_2, and C_x, converting the result back to admittance representation and adding the admittance matrix of the source–load capacitance C_{12}.

With the admittance matrix of the coupled SIRs given in [3] and assuming $C_1 = C_2 = C_0$ due to the symmetry of the circuit, the scattering parameters S_{11} and S_{21} of the filter are then given by

S_{11}

$$= \frac{\left(\frac{N}{M^2-N^2}+\omega C_{12}\right)^2 \frac{1}{Y_0^2} - \left(\frac{M}{M^2-N^2}-\omega C_{12}\right)^2 \frac{1}{Y_0^2}+1}{\frac{1}{Y_0^2}\left[\frac{1}{M^2-N^2}-\frac{2\omega C_{12}}{M-N}\right]+\frac{2j}{Y_0}\left[\frac{N}{M^2-N^2}+\omega C_{12}\right]+1} \quad (1)$$

S_{21}

$$= \frac{-2j\left[\frac{M}{M^2-N^2}-\omega C_{12}\right]\frac{1}{Y_0}}{\frac{1}{Y_0^2}\left[\frac{1}{M^2-N^2}-\frac{2\omega C_{12}}{M-N}\right]+\frac{2j}{Y_0}\left[\frac{N}{M^2-N^2}+\omega C_{12}\right]+1} \quad (2)$$

where Y_0 is the admittance of the connected lines at the input/output ports, and the other quantities are given by

$$M = \frac{Q - \omega C_i}{(Q - \omega C_i)^2 - (P + \omega C_i)^2}$$
$$+ \frac{\omega \frac{C_x}{2}}{\frac{1}{4}\omega^2 C_x^2 - \omega^2\left(C_o + \frac{1}{2}C_x\right)^2} \quad (3)$$

$$N = \frac{P + \omega C_i}{(Q - \omega C_i)^2 - (P + \omega C_i)^2}$$
$$+ \frac{\omega\left(C_o + \frac{1}{2}C_x\right)}{\frac{1}{4}\omega^2 C_x^2 - \omega^2\left(C_o + \frac{1}{2}C_x\right)^2} \quad (4)$$

$$Q = \left[\frac{k_o\alpha - k_e\beta - (\alpha + \beta)t^2}{2\alpha\beta t}\right] \quad (5)$$

$$P = \left[\frac{-k_o\alpha - k_e\beta + (\alpha + \beta)t^2}{2\alpha\beta t}\right] \quad (6)$$

where

$$k_e = \frac{Z_{e2}}{Z_{e1}}$$
$$k_o = \frac{Z_{o2}}{Z_{o1}}$$
$$\alpha = k_e(1 + k_e)Z_{e1}$$
$$\beta = k_o(1 + k_o)Z_{o1}$$
$$t = \tan\left(\frac{2\pi f\sqrt{\varepsilon_r}L_{1,2}}{c}\right).$$

$Z_{e/o}$ are the even/odd-mode impedances of the coupled-line resonator sections of lengths $L_1 = L_2$ [3], f is the frequency, and c is the speed of light.

The position of the attenuation poles is determined by letting $S_{21} = 0$ in (2).

In order to relate the dimensions of the actual structure to the quantities involved in the computation of (1) and (2), we use well-known expressions for the individual capacitances as outlined below.

A. Input and Output Capacitances

The input and output capacitances of the filter are estimated by using the thin-film capacitance model [6]. The capacitive pads are bent to miniaturize the structure, as well as to achieve the desired input and output capacitances. The capacitance between the pad and resonator beneath can be represented as a parallel combination of two capacitors (e.g., $C_1, C_2 = C_a + C_b$), as shown in Fig. 3.

The values C_a and C_b for the two sections shown in Fig. 3 are computed from

$$C_{a,b} = \frac{\varepsilon_r\varepsilon_0(l_{a,b} + \Delta f)(w_{a,b} + \Delta f)}{h} \quad (7)$$

where $l_{a,b}$ and $w_{a,b}$ are the lengths and widths of the two sections, respectively; h is the substrate thickness between the pad
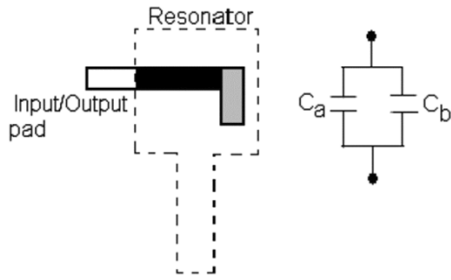
Fig. 3. Model to calculate input and output capacitances C_1, C_2; C_a and C_b refer to the dark and grey parts, respectively, on layer #3 [see Fig. 1(a)], which overlap with the resonator on layer #2.
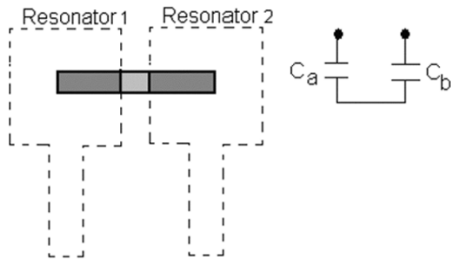
Fig. 4. Model to calculate the inter-resonator capacitance C_i.
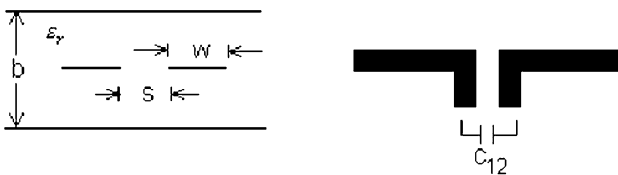
Fig. 5. Model to calculate the source–load capacitance C_{12}.

Fig. 6. Model to calculate the capacitances C_x between source and resonator 2, as well as resonator 1 and load.
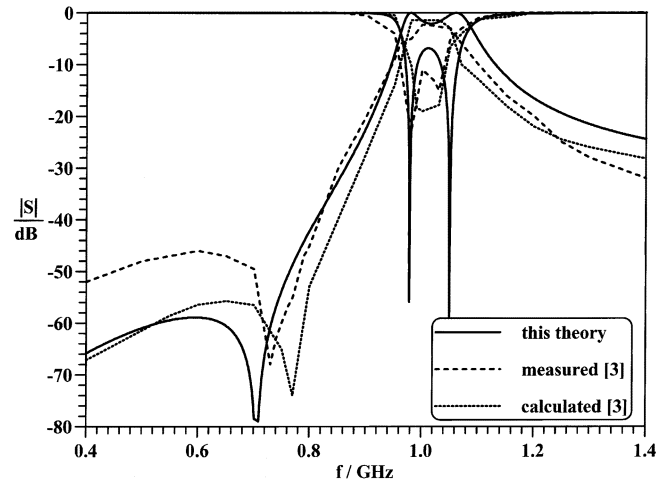
Fig. 7. Comparison between this theory and measurements, theory in [3] for an LTCC filter with an attenuation pole below the passband.

and resonator, and $\Delta f = 4h\ln(2)/\pi$ represents the fringing fields.

B. Inter-Resonator Capacitance

The inter-resonator capacitance can be represented as shown in Fig. 4. C_a and C_b are capacitances between resonators 1 and 2, respectively, and the strip. They are connected in series (i.e., $C_i = C_a C_b/(C_a + C_b)$) and can be estimated using the above thin-film capacitance model (7). These two capacitances are connected in series with the strip.

C. Source–Load Capacitance

This capacitance can be estimated by even- and odd-mode analysis of edge coupled striplines [6], as shown in Fig. 5. The total capacitance between the coupled lines is

$$C_{12} = \frac{C_0 - C_e}{2} l_{\text{eq}} \qquad (8)$$

where C_e and C_o are the even- and odd-mode capacitances [6], respectively, and l_{eq} is the total length of the edge-coupled lines including fringing fields.

D. Capacitance Between Source–Res2 and Res1–Load

The model to compute C_x is the offset-coupled stripline, as shown in Fig. 6.

The expression for C_x is identical to (8), but the even- and odd-mode capacitances are computed from the conformal mapping method in [7]. Since this technique holds only for striplines of identical width, we are applying, for simplicity, the average width between the feed line and resonator. l_{eq} is that part of the length of the feed line that is parallel to the resonator and includes fringing fields.

This averaging with respect to C_x is, of course, a limiting factor in the simplified analysis. Other limiting factors are, first, the validity range of closed-form expressions given, e.g., in [6] and, secondly, the fact that ground capacitances are neglected in favor of simplifying the approach. In other words, we expect our analysis to increase to deviate from the response of field solvers if the thicknesses of the upper and lower substrates in Fig. 1(a) decrease.

IV. RESULTS

In order to validate the simplified theory and demonstrate its applicability toward the design of miniaturized LTCC filters, we are comparing our results with measurements presented in [3].

Figs. 7 and 8 compare the measurements and computations of [3, Fig. 7(a) and (b)] with the results obtained with our method. For the capacitance and impedance values given in [3], our method predicts performances that are in good agreement with the measurements and computations in [3] for the two
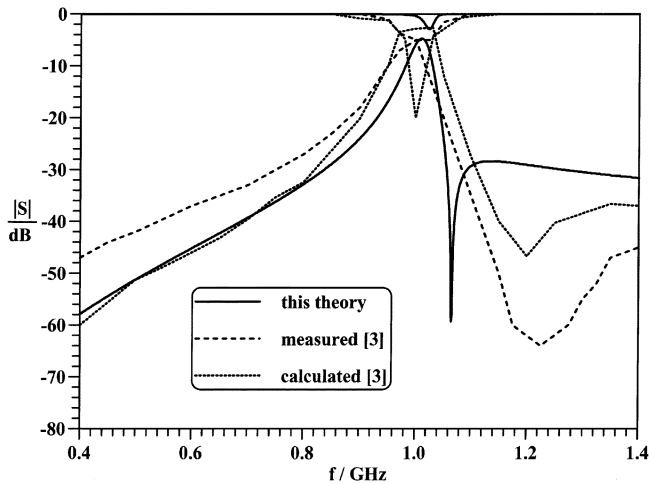
Fig. 8.   Comparison between this theory and measurements, theory in [3] for an LTCC filter with an attenuation pole above the passband.

cases showing an attenuation pole below (Fig. 7) and above (Fig. 8) the passband.

The difference between the two theoretical curves (solid and dotted lines) is caused by a number of factors. First, there are no actual dimensions given in [3] and, therefore, we used the capacitance and impedance values specified in [3]. Secondly, the coupling of the SIRs in [3] has been evaluated using a numerical technique, i.e., the spectral-domain approach, whereas we use the (much simpler) conformal-mapping expressions from [6] and [7]. Thirdly, the computation of capacitances is not specified in [3] and, most likely, differs completely from our simplified approach. Under such conditions, the results presented in Figs. 7 and 8 are in good agreement and verify our simplified approach.

We now apply this theory toward the design of the LTCC filter shown in Fig. 1. For given filter response specifications, the design starts with the generation/optimization of the coupling matrix according to [8] considering the fact that proximity coupled transmission lines are backward couplers, which defines positive coupling. The proximity of the SIRs usually creates a large positive coupling, which can be reduced by adding negative coupling via the capacitance C_i of the inter-resonator coupling pad. Note that the presence of C_i is essential in [3] to create a single transmission zero, whereas we are using it to control the coupling between the resonators, which mainly affects the bandwidth. From the coupling matrix and our equivalent-circuit approach, the capacitances can be calculated iteratively until the filter response is adequately represented.

For this design example, the center frequency is 945 MHz with attenuation poles at 620 MHz and 1.1 GHz. The dielectric material has $\varepsilon_r = 58$ and a total thickness of $b = 1.6$ mm, as shown in Fig. 1. The dimensions are as follows.

- *Layer #1* (inter-resonator coupling strip): width 0.2 mm, length 1.6 mm.
- *Layer #2* (SIR coupled lines): high-impedance section: length 3.2 mm, width 0.35 mm, gap 1.2 mm; low-impedance section: length 3.2 mm, width 1.55 mm, gap 0.2 mm.

(a)

(b)
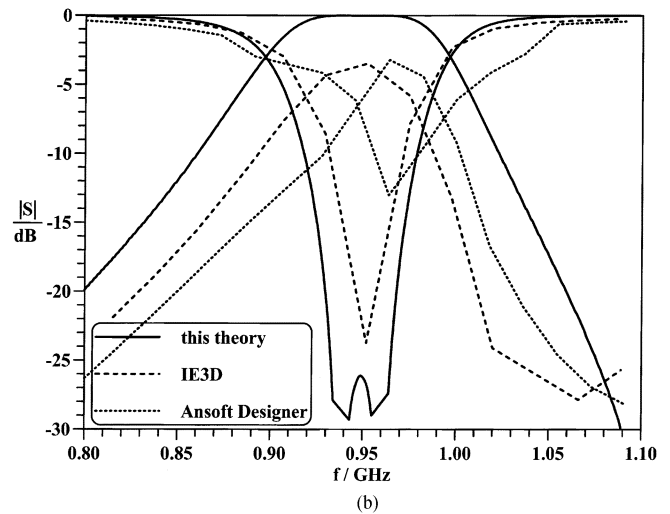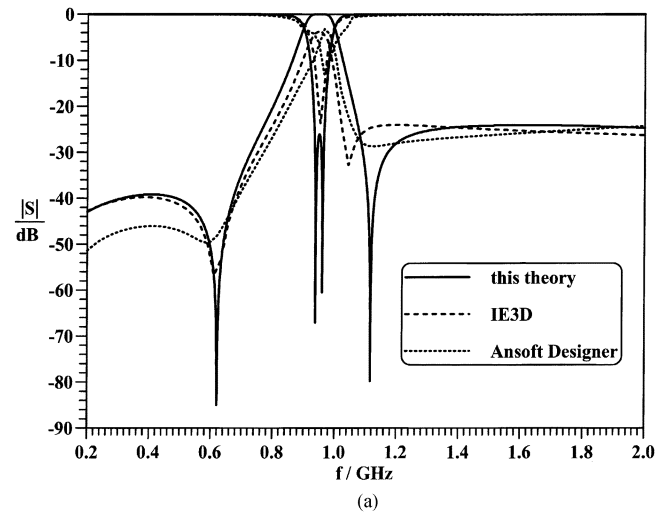
Fig. 9.   Comparison between results of simplified analysis and commercially available field solvers for a design according to Fig. 1. (a) Wide-band response. (b) Passband characteristics.

- *Layer #3* (L-shaped input/output pads, cf. Fig. 3): length for C_a: 1.3 mm, length for C_b: 0.5 mm. Widths of pads: 0.2 mm. Gap between pads: 0.3 mm.

These dimensions lead to the following parameters calculated from the theory: $Z_{e1} = 20$ Ω, $Z_{o1} = 18.6$ Ω, $Z_{e2} = 10$ Ω, $Z_{o2} = 7$ Ω, $C_1 = C_2 = 2.1$ pF, $C_i = (-)0.421$ pF, $C_{12} = (-)0.317$ pF, $C_x = (-)0.52$ pF. Note that the actually calculated capacitances are positive from the respective formulas in Section III. The negative signs in parentheses represent either negative coupling values due to the respective entry of the coupling matrix [8] or to create an admittance inverter [4]. This data results in the performance shown in Fig. 9(a) (theory), which is compared to full-wave solutions by the commercially available field solvers IE3D and Ansoft Designe. Very good agreement is obtained. Slight differences were to be expected because of the simplicity of the model.

Although the computations from the field solvers did not include losses, their predicted insertion losses are 3–4 dB and the passband is narrower [cf. Fig. 9(b)]. We attribute these losses to accessory electromagnetic coupling (and possible leakage) not included in the simplified theory. The level of attenuation in the

stopband matches with our theoretical predictions and presents an improvement compared to the design of [5]. We attribute this to the fact that our design uses all capacitive instead of both capacitive and inductive coupling in [5]. The locations of attenuation poles are predicted very well.

Since the CPU time is in extreme favor of this method (instant response versus approximately 30 min with IE3D and Designer for 100 frequency samples), it can be used to obtain a fast and reasonably accurate initial design. A fine optimization may then be performed with full-wave solvers.

V. CONCLUSIONS

The simplified analysis technique is a viable option for the design of capacitively coupled LTCC resonators. The individual capacitances introduced with this model account for the large majority of coupling effects between all elements of the filter. The theory compares well with previously published measurements. A new filter configuration with attenuation poles on either side of the passband has been initially designed and compares well with the results of field solvers. It has also presented a stopband improvement over similar state-of-the-art LTCC filters.

REFERENCES

[1] K. Lim, S. Pinel, M. Davis, A. Sutono, C.-H. Lee, D. Heo, A. Obatoynbo, J. Laskar, E. M. Tantzeris, and R. Tummala, "RF-system-on-package (SOP) for wireless communications," *IEEE Micro*, vol. 3, pp. 88–99, Mar. 2002.

[2] "World's smallest GSM front-end module in LTCC technology," EPCOS, Munich, Germany, news release, Jul. 2001.

[3] T. Ishizaki and T. Uwano, "A stepped impedance comb-line filter fabricated by using ceramic lamination technique," in *IEEE MTT-S Int. Microwave Symp. Dig.*, San Diego, CA, May 1994, pp. 617–620.

[4] T. Ishizaki, M. Fujita, H. Kagata, T. Uwano, and H. Miyake, "A very small dielectric planar filter for portable telephones," *IEEE Trans. Microw. Theory Tech.*, vol. 42, no. 11, pp. 2017–2022, Nov. 1994.

[5] L. K. Yeung and K.-L. Wu, "A compact second order LTCC bandpass filter with two finite transmission zeros," *IEEE Trans. Microw. Theory Tech.*, vol. 51, no. 2, pp. 337–341, Feb. 2003.

[6] B. C. Wadell, *Transmission-Line Design Handbook.* Boston, MA: Artech House, 1991.

[7] J. P. Shelton, "Impedance of offset parallel-coupled strip transmission lines," *IEEE Trans. Microw. Theory Tech.*, vol. MTT-14, no. 1, pp. 7–15, Jan. 1966.

[8] S. Amari, U. Rosenberg, and J. Bornemann, "Adaptive synthesis and design of resonator filters with source/load-multiresonator coupling," *IEEE Trans. Microw. Theory Tech.*, vol. 50, no. 8, pp. 1969–1978, Aug. 2002.

K. Rambabu received the Ph.D. degree from the University of Victoria, Victoria, BC, Canada, in 2004.

He has authored or coauthored 33 papers published in refereed journals and conferences. He holds a patent for beam shaping of a cellular base-station antenna. His research interests include design and development of miniaturized passive microwave components and antennas for various applications.

Jens Bornemann (M'87–SM'90–F'02) received the Dipl.-Ing. and Dr.-Ing. degrees in electrical engineering from the University of Bremen, Bremen, Germany, in 1980 and 1984, respectively.

From 1984 to 1985, he was a Consulting Engineer. In 1985, he joined the University of Bremen, as an Assistant Professor. Since April 1988, he has been with the Department of Electrical and Computer Engineering, University of Victoria, Victoria, BC, Canada, where he became a Professor in 1992. From 1992 to 1995, he was a Fellow of the British Columbia Advanced Systems Institute. In 1996, he was a Visiting Scientist with Spar Aerospace Limited (now EMS Technologies Inc.), Ste-Anne-de-Bellevue, QC, Canada, and a Visiting Professor with the Microwave Department, University of Ulm, Ulm, Germany. From 1997 to 2002, he was a Co-Director of the Center for Advanced Materials and Related Technology (CAMTEC), University of Victoria. In 2003, he was a Visiting Professor with the Laboratory for Electromagnetic Fields and Microwave Electronics, Eidgenössische Technische Hochschule (ETH) Zürich, Zürich, Switzerland. He coauthored *Waveguide Components for Antenna Feed Systems. Theory and Design* (Norwood, MA: Artech House, 1993) and has authored/coauthored over 200 technical papers. His research activities include RF/wireless/microwave/millimeter-wave components and systems design, and problems involving electromagnetic-field theory in integrated circuits, feed networks, and radiating structures. He serves on the Editorial Advisory Board of the *International Journal of Numerical Modeling*.

Dr. Bornemann is a Registered Professional Engineer in the Province of British Columbia, Canada. He serves on the Technical Program Committee of the IEEE Microwave Theory and Techniques Society (IEEE MTT-S) International Microwave Symposium (IMS). From 1999 to 2002, he was an associate editor of the IEEE TRANSACTIONS ON MICROWAVE THEORY AND TECHNIQUES in the area of microwave modeling and computer-aided design (CAD).